Journal of Materials Chemistry C

PAPER

View Article Online
View Journal | View Issue

Cite this: J. Mater. Chem. C, 2015, 3, 4545

New "X-type" second-order nonlinear optical (NLO) dendrimers: fewer chromophore moieties and high NLO effects†

Runli Tang,[a] Shengmin Zhou,[a] Wendi Xiang,[a] Yujun Xie,[a] Hong Chen,[a] Qian Peng,[b] Gui Yu,[b] Binwen Liu,[c] Huiyi Zeng,[c] Qianqian Li[a] and Zhen Li*[a]

Received 19th January 2015,
Accepted 27th March 2015

DOI: 10.1039/c5tc00182j

www.rsc.org/MaterialsC

New types of "X-type" NLO dendrimers, **C2** and **C3**, in which the chromophore moieties were arranged in order, were rationally designed. The special topology of the chromophore moieties contributed a great deal to the good NLO performance of **C2** and **C3**: the d_{33} value of **C2** (containing only five chromophore moieties) was 157.4 pm V^{-1}, while that of **C3** (containing nine chromophore moieties) achieved 195.2 pm V^{-1}, much larger than that of **C1** (74.7 pm V^{-1}, containing three chromophore moieties) and the fifth generation dendrimer (**G5**) (193.1 pm V^{-1}, bearing 62 pieces of chromophore moieties). Through careful experimental and theoretical analysis, their structure–property relationship was explained, and discussed in detail.

Introduction

Organic second-order nonlinear optical (NLO) material is a kind of advanced material with huge potential applications in photonic devices, such as high-speed electro-optic modulators, optical switches and frequency converters, which have been actively pursued with much impressive progress.[1] In the view of the molecular structure, chromophores with the donor–π–acceptor (D–π–A) structure are efficient components for NLO-active materials. To exhibit the macroscopic NLO effect, the chromophore moieties in organic NLO polymers should have an orderly noncentrosymmetric arrangement, which could be achieved from the natural symmetric alignment state by corona poling technique (Fig. 1).[2] However, the inherently strong dipole–dipole interactions among the chromophore moieties make their noncentrosymmetric alignment a daunting task during the poling process.[3] For this reason, how to efficiently transform the microscopic β value of chromophores to large macroscopic NLO activity of polymers becomes a major obstacle that hinders the rapid development of this field.

To decrease the strong dipole–dipole interactions, the direct method is to isolate the chromophore moieties by attaching some isolation groups, according to the "site isolation principle".[4] Based on the excellent work of other scientists, we have synthesized different types of polymers, and proposed the concept of a "suitable isolation group"[5] for the rational design of NLO polymers (Fig. 1). Accordingly, for the normal azo benzene chromophore with three isolation groups around it, the suitable isolation group should be the triazole ring, which could be conveniently constructed from the powerful click chemistry reaction.[6] For example, with the presence of the triazole rings

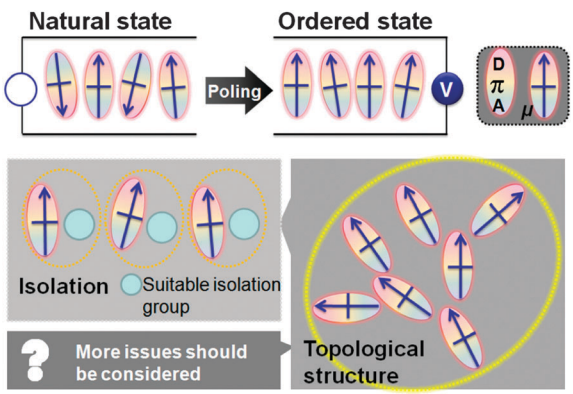

Fig. 1 The poling process required to demonstrate the macroscopic NLO effect and issues considered to help the design of NLO polymers.

[a] Department of Chemistry, Wuhan University, Wuhan 430072, China. E-mail: lizhen@whu.edu.cn, lichemlab@163.com; Fax: +86 027 68755363
[b] Institute of Chemistry, the Chinese Academy of Sciences, Beijing 100080, China
[c] Fujian Institute of Research on the Structure of Matter, the Chinese Academy of Sciences, Fuzhou 350002, China

† Electronic supplementary information (ESI) available: The structures of dendrimers **Gn** (n = 1–5), global-like dendrimers **Gn-TPA** (n = 1–3), and related parameters; the synthesis of compounds; NLO measurements including NLO coefficient theories, preparing thin films, measurement conditions, stability and error analysis; DFT calculation method for IR spectra; molecular mechanics simulation including calculation method, results and discussion; NMR spectra, TOF mass spectra, UV-vis spectra, TGA thermograms; optimized structures of **Frag1–Frag3** by DFT method; optimized structures of **C1–C3**, **G1–G2** by MM simulation and DFT method. See DOI: 10.1039/c5tc00182j

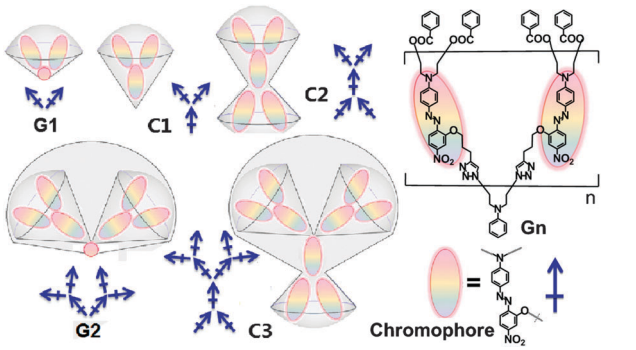

Fig. 2 The spatial structural diagram and the corresponding two-dimensional dipole moments of **C1**, **C2**, **C3** and **Gn**.

acting as suitable isolation groups, accompanied with the increasing generation of dendrimers, from **G1** to **G5** (Fig. 2 and Scheme S1, ESI†), the measured NLO coefficient increased from 122.7 (**G3**) to 177.0 (**G4**), then to 193.1 pm V^{-1} (**G5**), confirming that the frequently observed asymptotic dependence of electro-optic activity on the chromophore number density may be overcome through rational design, according to the concept of a "suitable isolation group".[7]

Except for the introduction of a "suitable isolation group", another parameter, having enough room for the alignment of chromophores upon poling, is also very important to achieve large macroscopic NLO effects, which was concerned with the topological structure of the polymers. Actually, from this point, Jen, Dalton, and co-workers have put forward the idea that high macroscopic NLO efficiency could be achieved when treating chromophore moieties as spheres.[8] Previously, we have prepared many dendrimers, hyperbranched polymers, star-type macromolecules, with good NLO performance. Among them, similar to the reported cases in the literature,[1,2] dendrimers possess many amazing properties and are considered to be the most promising candidates for the next generation of NLO materials. However, most of the dendrimers have a conical shape, not an exactly spherical one. Thus, we have tried to control their shape by using triphenyl amine as the core, to yield the so called "global-like dendrimers" (Scheme S1, ESI†).[9] Although they demonstrated better NLO performance, they are still not as effective as a sphere.

With the purpose of designing more sphere-like dendrimers, and diversifying their topological structure, in this work a new kind of dendrimer (**C1**, **C2** and **C3**) was designed, in which **C2** and **C3** shared the same framework of "X-type" structure (Fig. 2). As mentioned above, the triazole rings were utilized as the suitable isolation groups in **C1**, **C2** and **C3**, to decrease the strong dipole–dipole interactions. In addition to the more spherical shape in particular, the dipole moments of the chromophore moieties in these molecules were designed to be naturally aligned in a certain direction, to construct a microscopic noncentrosymmetric topological structure, which should be beneficial to the orientation of the chromophore moieties during the poling process, for the further enhancement of their macroscopic NLO effects. Excitingly, the d_{33} value of **C2** was tested to be 157.4 pm V^{-1}, and the d_{33} value of **C3** with only nine pieces of azo benzene chromophore moieties, was as high as 195.2 pm V^{-1}, a little higher than that of **G5** bearing 62 chromophore ones. The theoretical calculations confirmed the advantages of this X-type structure. Herein, we would like to present the synthesis, characterization, calculations and NLO properties of **C1**, **C2** and **C3** in detail.

Results and discussion

Synthesis

Compounds **C1**, **C2** and **C3** shared a similar synthetic method through the highly-effective, Cu(I)-catalyzed 1,3-dipolar cycloaddition reaction between azides and alkynes (the Sharpless "click" reaction).[10] **C1** was easily obtained from compound **2** and **S2**, for its simple one-dimension-upward "Y-type" structure. However, **C2** and **C3** possessed an "X-type" structure, thus, a suitable linkage part (compound **4**) and a rational synthetic approach should be carefully chosen. As shown in Chart 1 and Scheme 1, the converge-then-diverge approach was utilized to synthesize **C2** and **C3**. Compound **4**, which possessed two alkyne groups (reactive groups for the azido moieties in compound **2**) at the tail and two chlorine atoms (for further functionalized in the next step) at the head, served as the linkage part, to yield compound **6** using the convergent approach. Then, after the conversion of chlorine atoms of compound **6** into the azido ones of compound **1**, through the divergent approach, compound **1** reacted with different alkyne-functional compounds to conveniently afford **C2** and **C3**.

The synthetic route to **C1**–**C3** is demonstrated in Scheme 1, and the synthesis of some intermediates is presented in the ESI,† while **G1**≡ was prepared according to our previous work.[7] Thus, the whole synthetic procedure to **C1**, **C2** and **C3** was convenient, with satisfactory yields. All the target molecules were soluble in common organic solvents, such as dichloromethane, chloroform, THF, and their solutions could be easily spin-coated into thin solid films. Therefore, it was convenient to measure their NLO and other properties both in solutions and thin films.

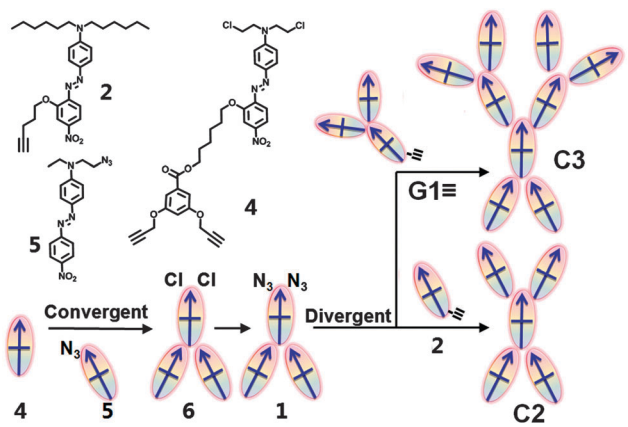

Chart 1 The synthetic route: converge-then-diverge approach.

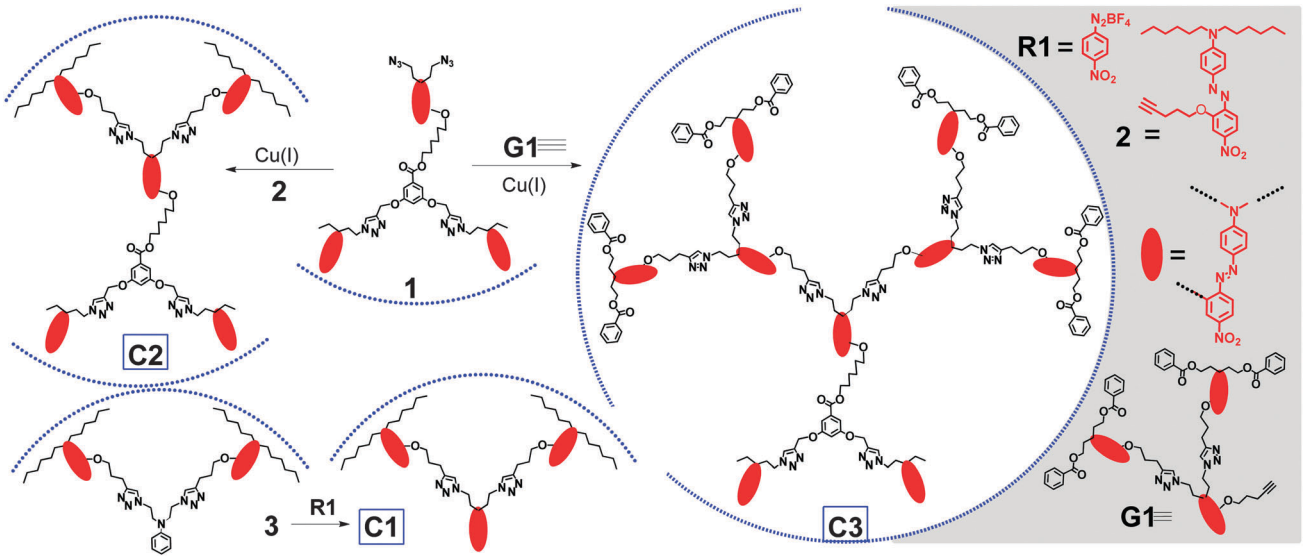

Scheme 1 The synthetic route of **C1**, **C2** and **C3**.

Characterizations

The prepared **C1–C3** and other related compounds were well characterized by using the spectroscopic method, including Fourier transforming infrared spectrum (FT-IR), nuclear magnetic resonance (NMR), UV-vis spectroscopy, thermogravimetric analysis (TGA), differential scanning calorimetry (DSC), elemental analysis (EA), and MALDI-TOF mass spectrometry. All gave satisfactory data (see Experimental section and ESI† for detailed analysis data). Among them, the vibrational spectral study was basically used for the structure characterization. For new molecules, especially for macromolecules, it was not easy to describe the original and intricate vibrational spectral properties in experiments. Herein, the density functional theory (DFT) calculation did help, which has been widely used for the study of NLO active compounds.[11] Moreover, the fragment approach provided an effective way to reduce the computational times with enough accuracy for large systems.[12] Based on DFT, we simulated the FT-IR spectra of **C1**, **C2** and **C3**, by using the fragment method. **C1**, **C2** and **C3** were broken into three fragments: **Frag1**, **Frag2**, and **Frag3**, respectively (their optimized structures are shown in the ESI†).

Fig. 3 shows the chemical structures of these three fragments, and calculated the FT-IR spectra of **Frag1**, **Frag2**, **Frag3**, and experimental ones of **C1**, **C2**, **C3**. From the spectra, it was easily seen that the calculation results matched well to the experimental ones. The absorption region of 3000–2800 cm^{-1} originated from the asymmetrical and symmetrical stretching bands of the methylene groups. The peak at 1716 cm^{-1} (peak#) in the spectrum of **C3** was found to be at 1680 cm^{-1} in those of **Frag1** and **Frag2**, which should be attributed to the stretching mode of C=O from ester groups. As there were no ester groups in **C1**, but nine ones in **C3**, peak# was only found in the spectrum of **C3**. The same case occurred for peak*, the out-of-plane ring bend vibration of benzene (ROCOPh-H), which was found at 714 cm^{-1} in both the experimental and calculation results. Since **C3** had

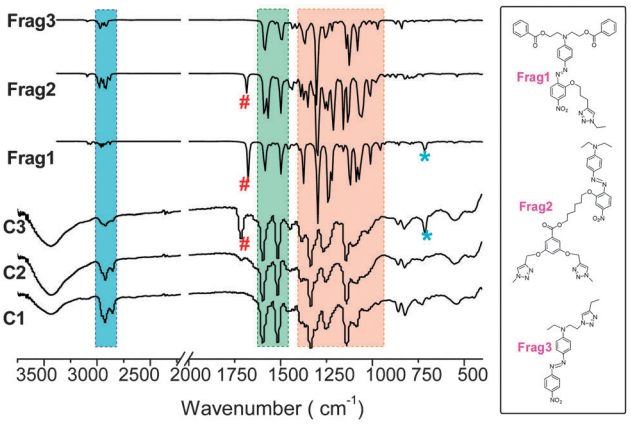

Fig. 3 FT-IR spectra (left) of **Frag1**, **Frag2**, **Frag3** (calculated results) and **C1**, **C2**, **C3** (experimental results); chemical structure of Frags (right).

eight groups of ROCOPh-H, a moderate intensity of peak* was observed. Labelled as the green region, the peaks at 1595 and 1515 cm^{-1} originated respectively from the asymmetrical and symmetrical stretching of Ph-Azo-Ph and Ph-Azo-Ph-NO_2. However, the peaks in the yellow region (1400–950 cm^{-1}) were mainly ascribed to the in-plane stretching and rocking vibration of chromophore moieties (N-Ph-Azo-Ph-NO_2) and its linked alkyl chain. Intuitively, the absorption bands associated with the carbonyl groups (1716 cm^{-1}) and nitro groups (1337 and 1515 cm^{-1}) in their FT-IR spectra partially confirmed that the chromophore moieties were stable during the synthetic process.

Although the calculation-assisted FT-IR spectroscopy provided detailed structural characteristics, it was far from enough. Thus, NMR spectroscopic analysis, including ^{1}H-NMR and ^{13}C-NMR analysis, was conducted, to identify the structure of the target compounds and intermediates (the Experimental section in the ESI† for detailed analysis data and spectra). MALDI-TOF mass spectrometry was used to confirm the exact molecular weight,

Table 1 Characterization data

No.	Yield (%)	m/z^a	m/z(cal)^b	$T_g{}^c$ (°C)	$T_d{}^d$ (°C)
C1	81.2	1388.0	1387.7	—	285
C2	74.4	2395.9	2395.2	84	310
C3	63.7	4813.0	4815.7	98	287

[a] Measured by MALDI-TOF mass spectroscopy. [b] Calculated for $[M + Na]^+$. [c] Glass transition temperature (T_g) detected by DSC analysis under argon at a heating rate of 10 °C min^{-1}. [d] The 5% weight loss temperature of polymers detected by TGA analysis under nitrogen at a heating rate of 10 °C min^{-1}.

Table 2 The maximum absorption wavelength (λ_{max}, nm) in different solvents (0.02 mg mL^{-1})

	1,4-Dioxane	CH_2Cl_2	$CHCl_3$	THF	DMF	DMSO	Film
C1	463	474	466	470	487	494	481
C2	465	477	471	476	492	498	480
C3	458	458	458	463	477	483	468

and all the experimental results were in good agreement with the expected molecular weights for the structures (Table 1). The dendrimers were thermally stable, as shown in Table 1 and Fig. S35 (ESI†); the degradation temperatures (T_d) for the dendrimers were higher than 280 °C. The glass transition temperatures (T_g) of the dendrimers were also investigated using differential scanning calorimetry (DSC) (Table 1).

The UV-vis absorption spectra of these compounds were measured in different solvents. Their maximum absorption wavelengths for the $\pi \rightarrow \pi^*$ transition of the azo moieties are listed in Table 2, and Fig. 4 shows the UV-vis spectra of the three molecules in solutions (THF) and thin films; the detailed UV-vis spectra are presented in the ESI.† All the compounds

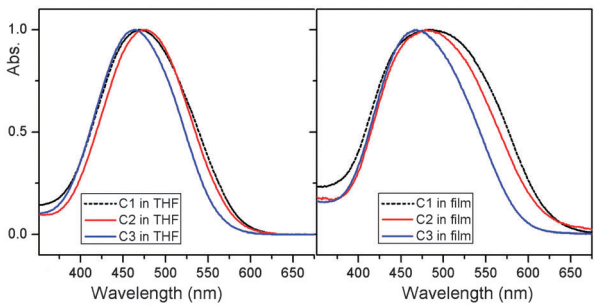

Fig. 4 The UV-vis spectra of **C1**, **C2**, **C3** in THF solvent (left) and in thin films (right).

demonstrated solvatochromism phenomena, for **C1** and **C2** the difference of λ_{max} was about 30 nm from the low polar solvent to the high polar one, because of the lower number of contained chromophore moieties (easily affected by solvents), while for **C3**, with a small increase in the number of the chromophore moieties, this difference decreased to 25 nm. In addition, the λ_{max} of **C3** was blue-shifted in comparison with those of **C1** and **C2**, due to their different chemical structures, that is, the main electron donor of **C1** and **C2** was *N*,*N*-dihexylaniline, which is a strong electron donor, while that of **C3** was a substituted aniline group by ethyl benzoate, a slightly weaker donor than *N*,*N*-dihexylaniline. In this case, the difference between **C1** and **C2** was understandable. The λ_{max} of **C2** was slightly red-shifted in dilute solutions, in comparison with that of **C1**, while they were almost the same in the films. Meanwhile, the absorption peak of **C1** was a little wider and more red-shifted than that of **C2**, indicating that the inhibition of solid aggregation is better in **C2**.

NLO properties

To evaluate the NLO activities of **C1**, **C2** and **C3**, their poled thin films were prepared by spin-coating. One of the most convenient techniques to study the second-order NLO activity is to investigate the second harmonic generation (SHG) process, which was characterized by an SHG coefficient (d_{33}). The method for the calculation of d_{33} values of the poled films has been discussed in the ESI† and reported in our previous papers.[5] The d_{33} value of each dendrimer was calculated by averaging the testing values of repeated measurements, including that of the same film and different films of a specific molecule (the testing stability and error analysis were discussed in the ESI†). The NLO coefficients of these three dendrimers are listed in Table 3, with other related parameters. Generally, the d_{33}@1064 value tested under the 1064 nm fundamental beam was researched as the main parameter in our previous work, as the 1064 nm laser showed broad applications in research and technology. From the experimental data, the d_{33}@1064 values of **C2** and **C3** were tested to be 157.4 and 195.2 pm V^{-1}, respectively, while on the same measurement system, it was only 74.7 pm V^{-1} for **C1**. Also, the d_{33}@1950 value was tested under the 1950 nm fundamental beam. The d_{33}@1950 value of **C1** was 17.1 pm V^{-1}, while 39.7 pm V^{-1} for **C2**, and 53.6 pm V^{-1} for **C3**. The d_{33}@1950 values were smaller than the d_{33}@1064 ones, because of the dispersion of d_{33} of the poled films.[13] Both d_{33}@1950 and d_{33}@1064 showed the same trend. In order to subtract out the impact of the fundamental beam, the $d_{33(\infty)}$ values were calculated using the approximate two-level model

Table 3 The NLO properties of dendrimers

No.	$T_e{}^a$ (°C)	$l_s{}^b$ (nm)	$d_{33}{}^c$@1064 (pm V^{-1})	$d_{33(\infty)}{}^d$@1064 (pm V^{-1})	$d_3{}^c$@1950 (pm V^{-1})	$d_{33(\infty)}{}^d$@1950 (pm V^{-1})	Φ^e	N^f (%)
C1	39	289 ± 3.1	74.7 ± 8.2	10.7 ± 1.1	17.0 ± 1.8	12.1 ± 1.3	0.19	0.55
C2	80	227 ± 3.1	157.4 ± 17.2	23.2 ± 2.6	39.7 ± 4.5	28.3 ± 3.2	0.20	0.47
C3	100	212 ± 3.1	195.2 ± 22.3	35.5 ± 4.0	53.6 ± 6.1	38.9 ± 4.4	0.19	0.55

[a] The best poling temperature. [b] Film thickness. [c] Second harmonic generation (SHG) coefficient. [d] The nonresonant d_{33} values calculated by using the approximate two-level model. [e] Order parameter $\Phi = 1 - A_1/A_0$, A_1 and A_0 are the absorbance of the polymer film after and before corona poling, respectively. [f] The loading density of the effective chromophore moieties.

(ESI†). The $d_{33(\infty)}$@1064 values of **C1**, **C2** and **C3**, tested under the 1064 nm laser, were 10.7, 23.2, and 35.5 pm V^{-1} respectively, while the corresponding $d_{33(\infty)}$@1950 values were 12.1, 28.3, and 38.9 pm V^{-1}, respectively. The small difference in the $d_{33(\infty)}$@1064 and $d_{33(\infty)}$@1950 values might be caused by the extra UV-vis absorption: the UV-vis absorption edges of the three compounds crossed 532 nm (UV-vis absorption spectra in solvents and films, ESI†). In other words, the frequency doubling light might cause little loss to the UV-vis absorption.

From **C1** to **C2**, the number of chromophore moieties went from just three to five, while the loading density of the effective chromophores (N) decreased from 0.55 to 0.47. However, the d_{33} value increased rapidly, with the d_{33}@1064 value increasing from 74.7 to 157.4 pm V^{-1}, and the $d_{33(\infty)}$@1064 value increased from 10.7 to 23.2 pm V^{-1}. This phenomenon raised a question: why does **C2** show such a big improvement in the d_{33} value in comparison with **C1**?

Analyzing the structure carefully, **C2** was equal to one **C1** with two additional chromophore moieties on the tail through covalent bonds. Perhaps these covalent bonds made some sense in that they could aid the arrangement of the five chromophore moieties of **C2** in orderly rows, rather than the normal disordered stacking ones. To partially confirm this point, a control experiment was conducted. As shown in Scheme 2, **C2** could be considered to be composed of two parts, similar to those of **C1** and **C4** (the synthesis and characterization data are presented in the ESI†). Thus, a mixture of compound **C1** and **C4** was prepared at a molar ratio of 1 : 1.

From the SHG measurement, the d_{33}@1064 value of the **C1**/**C4** mixture was tested to be 71 pm V^{-1}, even lower than that of **C1** itself, under the best poling temperature of 34 °C. However, once the piece of **C4** was bonded onto **C1** as a tail, the d_{33}@1064 value of the resultant **C2** was as high as 157.4 pm V^{-1}, more than double that of **C1**. The difference could also be observed clearly in the de-poling process. Fig. 5 shows the de-poling curves of **C2**, **C1** and the **C1**/**C4** mixture. The **C1**/**C4** mixture showed the poorest performance, once again indicating the importance of the covalent bonds. Compared to that of **G3** (Scheme S1, ESI†), this value was still very high, no matter that there were 14 chromophore moieties in **G3** but only 5 in **C2**. Thus, the covalent

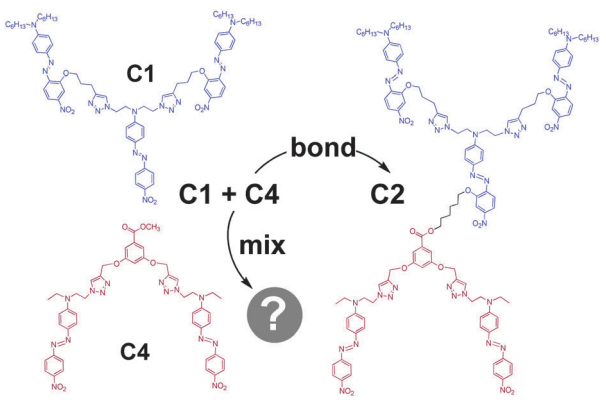

Scheme 2 Structures of **C1**, **C2** and **C4**.

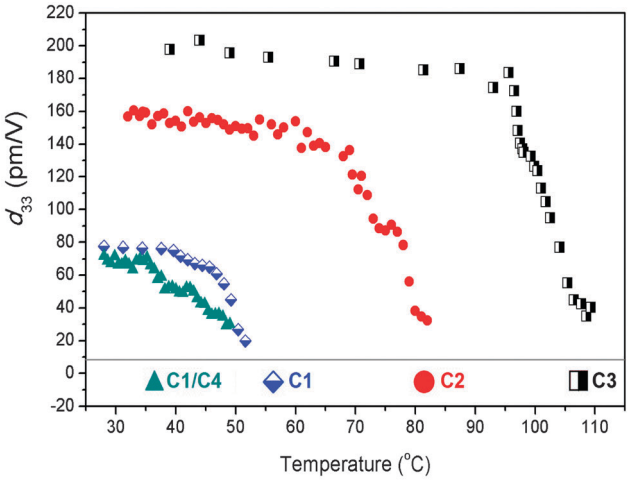

Fig. 5 De-poling curve of **C3**, **C2**, **C1** and **C1**/**C4** (measured at 1064 nm fundamental beam).

linkage should not be the only reason for the high NLO effect of **C2**. To gather more information, additional chromophore moieties were further introduced to the head of **C2**, not only limited to the tail part, to construct a new dendrimer, **C3**, in which there were nine chromophore moieties in total. Excitingly, the d_{33}@1064 value of **C3** was tested to be as high as 195.2 pm V^{-1}, even higher than that of **G5** bearing 62 pieces of chromophore moieties (Scheme S1, ESI†). Analyzing the structures of **C2** and **C3** carefully, it seemed that there was no big difference from those of **G1–G5**, except the presence of one benzene ring as the additional isolation group. As mentioned in the introduction part, we have designed so called "global-like dendrimers" (Scheme S1, ESI†), which exhibited higher NLO effects than those of **G1–G5**, disclosing the importance of the perfect 3D structure of the dendrimers.

However, it was really hard to make it clear how the molecular conformation affected the macroscopic coefficient, as it faced at least three large hurdles: first, the real conformation of the single molecule, especially for such macromolecular dendrimers; secondly, the stacking model of molecules in thin films; and third the conformation of the ordered molecules in the poled films. Actually, even the first one had not been fully understood; for some NLO effective macromolecules, no direct data of spatial structure from the crystal has been obtained so far. In most cases, we reduced the intermediate link but only observed the original chemical structure and the resultant efficiency. In this work, we made an attempt to obtain the single molecular conformation by using molecular mechanics simulation. We performed a molecular mechanics simulation for **C1**, **C2**, **C3**, and also for **G1** and **G2** for comparison (the calculation method, results and discussion are presented in the ESI†). The results showed that **C1** and **G1** had similar conformations: approximately planar, and all the chromophore moieties were exposed to the interface, possibly leading to a strong interaction of the electrical dipole moments. This was supposed to be the main reason for their low NLO effects. In contrast, other molecules exhibited 3D-extended conformations.

In particular, the conformation of **C3** was almost spherical, providing a good candidate conformation to achieve a large NLO effect. Molecular mechanics simulation was a good way to help obtain more microcosmic information, even the single molecular conformation was only the tip of an iceberg; a better response program to the second and third hurdles was then expected.

Conclusions

In summary, three dendrimers, **C1**, **C2** and **C3**, were successfully synthesized and carefully investigated. **C2** and **C3** were designed as an "X-type" structure, with the chromophore moieties being arranged partially in order, which was a better structure for good NLO efficiency. As a result, **C2** and **C3** exhibited large NLO effects, with d_{33} values as high as 157.4 and 195.2 pm V^{-1}, no matter that there were only five or nine chromophore moieties in them, respectively. Through the control experiments and some theoretical calculations, it was found that **C2** and **C3** had 3D-extended conformations, and their chromophore moieties were well oriented in nature. For **C3**, its conformation was almost spherical, the best conformation to achieve a large NLO effect. It is believed that by further modifying the chemical structure more intelligently, even better performance could be achieved with the utilization of the very simple azo chromophore moieties.

Experimental

Instrumentation

^{1}H and ^{13}C NMR spectra were measured on a Varian Mercury300, Bruker ARX400, or Bruker BioSpin GmbH spectrometer using tetramethylsilane (TMS; δ = 0 ppm) as the internal standard. UV-visible spectra were obtained using a Schimadzu UV-2550 spectrometer. The Fourier transform infrared (FTIR) spectra were recorded on a Perkin Elmer-2 spectrometer in the region 3000–400 cm^{-1} on KBr pellets. Elemental analysis was performed on a CARLOERBA-1106 micro-elemental analyzer. A MALDI-TOF mass spectrometer (MALDI-TOF MS; ABI, American) equipped with a 337 nm nitrogen laser and a 1.2 m linear flight path in positive ion mode. Thermal analysis was performed on a NETZSCH STA449C thermal analyzer at a heating rate of 10 °C min^{-1} in nitrogen at a flow rate of 50 cm^3 min^{-1} for thermogravimetric analysis (TGA). The thermal transitions of the polymers were investigated using a METTLER differential scanning calorimeter DSC822e under nitrogen at a scanning rate of 10 °C min^{-1}. The thermometer for measurement of the melting point was uncorrected. The thickness of the films was measured with an Ambios Technology XP-2 profilometer.

Preparation of thin films

The samples were dissolved in THF (concentration ~3 wt%), and the solutions were filtered through syringe filters. The thin films were spin-coated onto indium-tin-oxide (ITO)-coated glass substrates, which were subjected to ultrasonication in different solvent systems including 2% soap in water, acetone, deionized water, DMF, THF. Each step was carried out for 20 min. The residual solvent of the thin films was removed by heating the films in a vacuum oven at 45 °C.

Measurement condition

The second-order optical nonlinearity of the materials was determined by *in situ* second harmonic generation (SHG) experiment by using a closed temperature-controlled oven with optical windows and three needle electrodes. The films were kept at 45° to the incident beam and poled inside the oven, and the SHG intensity was monitored simultaneously. Poling conditions were as follows: temperature, different for each polymer (Table 3); voltage, 7.0 kV at the needle point; gap distance, 0.8 cm. The SHG measurements were carried out with a Nd:YAG laser operating at a 10 Hz repetition rate and an 8 ns pulse width at 1064 nm. The stability and error of the system is analyzed in the ESI.†

The NLO efficiencies were also investigated using 1950 nm laser radiation. The doubled frequency signals (975 nm) were detected by an Andor's DU420A-BR-DD CCD after the mixed signals passed through the monochromator.

Synthesis

C1: compound **3** (121.6 mg, 0.1 mmol) and compound **R1** (35.6 mg, 0.15 mmol) were dissolved in DMF (10 mL). After stirring for 24 h at 0 °C, the mixture was poured into a lot of ice water, and some sodium bicarbonate was added to adjust the pH to ~7.0. The deep red precipitate was filtered, washed with water, and purified by column chromatography on silica gel using chloroform/petroleum ether (3/1) as the eluent to afford a red solid (110.8 mg, 81.2%). ^{1}H NMR (300 MHz, $CDCl_3$, 298 K), δ (TMS, ppm): 0.90 (br, s, 12H, $-CH_3$), 1.32 (br, s, 24H, $-CH_2-$), 1.62 (br, s, 16H, $-CH_2-$), 2.23 (t, J = 7.2 Hz, $-CH_2-$), 2.96 (t, J = 6.6 Hz, $-CH_2-$), 3.35 (t, J = 7.2 Hz, 8H, $-CH_2-$), 3.71 (t, J = 6.6 Hz, $-CH_2-$), 4.13 (t, J = 6.0 Hz, $-CH_2-$), 4.36 (br, s, 4H, –CH2), 6.53 (d, J = 8.4 Hz, 2H, $-CH_2-$), 6.67 (br, 4H, ArH), 7.23 (s, 3H, ArH), 7.85–7.62 (m, 11H, ArH), 8.27 (d, J = 7.8 Hz, 2H, ArH). ^{13}C NMR (100 MHz, $CDCl_3$, 298 K), δ (ppm): 154.72, 151.42, 149.31, 147.58, 147.20, 144.50, 143.71, 139.24, 126.32, 125.95, 124.47, 122.74, 122.35, 117.11, 116.52, 113.37, 111.48, 111.06, 109.11, 68.41, 51.20, 47.11, 31.54, 28.27, 28.21, 27.23, 26.63, 22.56, 21.75, 14.80, 13.95, MALDI-TOF MS: calcd for ($C_{74}H_{96}N_{18}O_8$): m/z $[M + Na]^+$: 1387.7; found: m/z 1388.0. (EA) (%, found/calcd): C, 65.02/65.08; H, 6.83/7.09; N, 18.34/18.46.

C2: compound **1** (138.7 mg, 0.10 mmol), compound **2** (103.4 mg, 0.21 mmol), $CuSO_4{\cdot}5H_2O$ (10 mol%), $NaHCO_3$ (20 mol%), and ascorbic acid (20 mol%) were dissolved in DMF (8 mL)/H_2O (1 mL) under nitrogen in a Schlenk flask. The mixture was stirred at 30 °C overnight, then extracted with chloroform, and washed with 1 N HCl, 1 N NH_4OH and then water. The organic layer was dried over anhydrous magnesium sulfate. After removal of the solvent, the crude product was purified by column chromatography using THF/chloroform (1/8) as the eluent to afford a deep red solid (176.4 mg, 74.4%). ^{1}H NMR (300 MHz, $CDCl_3$, 298 K), δ (TMS, ppm): 0.89 (br, s, 12H, $-CH_3$), 1.08 (t, J = 6.6 Hz, 6H, $-CH_3$), 1.31 (br, s, 24H, $-CH_2-$), 1.79

(br, s, 4H, $-CH_2-$), 1.94 (br, s, 4H, $-CH_2-$), 2.21 (t, J = 6.6 Hz, 4H, $-CH_2-$), 2.94 (t, J = 6.3 Hz, 4H, $-CH_2-$), 3.21 (m, 4H, $-CH_2-$), 3.34 (m, 8H, $-CH_2-$), 3.69 (br, s, 4H, $-CH_2-$), 3.92 (br, 4H, $-CH_2-$), 4.11 (br, 4H, $-CH_2-$), 4.20 (br, 2H, $-CH_2-$), 4.27 (br, 2H, $-CH_2-$), 4.36 (br, 4H, $-CH_2-$), 4.59 (br, 4H, $-CH_2-$), 5.12 (s, 4H, $-CH_2-$), 6.58 (d, J = 9.0 Hz, 2H, ArH), 6.66 (m, 8H, ArH), 6.74 (br, s, 2H, ArH), 7.16 (br, s, 2H, ArH), 7.29 (br, 2H, ArH), 7.59 (m, 4H, ArH), 7.74–7.72 (m, 4H, ArH), 7.89–7.80 (m, 16H, ArH), 8.28 (m, 4H, ArH). ^{13}C NMR (75 MHz, THF-d_8, 298 K), δ (ppm): 160.53, 157.57, 156.45, 152.46, 152.01, 149.08, 148.66, 147.99, 147.60, 145.06, 144.37, 133.43, 127.00, 125.41, 125.14, 123.47, 123.09, 117.66, 116.86, 112.44, 112.11, 110.24, 109.49, 107.12, 70.68, 69.62, 68.03, 67.73, 67.44, 67.15, 66.86, 62.89, 51.92, 51.16, 48.23, 47.80, 46.32, 32.71, 29.79, 28.32, 27.63, 26.80, 25.89, 25.62, 25.36, 25.09, 24.83, 23.63, 22.68, 14.44, 12.38. MALDI-TOF MS: calcd for ($C_{125}H_{150}N_{32}O_{17}$): m/z [M + Na]$^+$: 2395.2; found: m/z 2395.9. (EA) (%, found/calcd): C, 63.10/63.27; H, 6.20/6.37; N, 18.74/18.89.

C3: compound **1** (34.6 mg, 0.02 mmol), **G1**≡ (93.7 mg, 0.55 mmol), $CuSO_4{\cdot}5H_2O$ (10 mol%), $NaHCO_3$ (20 mol%), and ascorbic acid (20 mol%) were dissolved in DMF (8 mL)/H_2O (0.8 mL) under nitrogen in a Schlenk flask. The mixture was stirred at 30 °C overnight, then extracted with chloroform, and washed with 1 N HCl, 1 N NH_4OH and then water. The organic layer was dried over anhydrous magnesium sulfate. After removal of the solvent, the crude product was purified by column chromatography using THF/chloroform (1/3) as the eluent to afford a deep red solid (152.6 mg, 63.7%). ^{1}H NMR (300 MHz, $CDCl_3$, 298 K), δ (ppm): 1.04 (t, J = 6.9 Hz, 6H, $-CH_3$), 1.25 (br, 2H, $-CH_2-$), 1.90 (br, 2H, $-CH_2-$), 1.92 (br, 2H, $-CH_2-$), 2.19 (br, 12H, $-CH_2-$), 2.91 (br, 12H, $-CH_2-$), 3.19 (m, 4H, $-CH_2-$), 3.69 (m, 12H, $-CH_2-$), 3.90 (br, s, 16H, $-CH_2-$), 4.09 (br, s, 12H, $-CH_2-$), 4.24 (m, 4H, $-CH_2-$), 4.36 (m, 12H, $-CH_2-$), 4.54 (br, 16H, $-CH_2-$), 5.11 (s, 4H, $-CH_2-$), 6.48 (m, 4H, ArH), 6.65–6.62 (m, 8H, ArH), 6.93–6.91 (m, 8H, ArH), 7.15 (s, 2H, ArH), 7.28 (br, s, 4H, ArH), 7.84–7.37 (m, 24H, ArH), 7.98–9.96 (m, 16H, ArH), 8.23 (m, 4H, ArH). ^{13}C NMR (75 MHz, THF-d_8, 298 K), δ (ppm): 166.79, 166.46, 160.55, 157.57, 156.79, 156.70, 156.61, 152.37, 152.03, 151.27, 149.59, 149.44, 148.64, 147.73, 147.45, 147.35, 146.12, 145.96, 144.95, 144.41, 133.92, 133.45, 131.09, 130.41, 129.33, 127.03, 126.85, 126.75, 125.43, 125.28, 123.50, 123.25, 117.87, 116.86, 112.98, 112.60, 112.47, 110.32, 109.53, 107.20, 70.71, 69.70, 68.08, 67.78, 67.49, 67.20, 66.91, 65.86, 62.91, 51.97, 51.19, 50.58, 48.30, 47.92, 46.37, 30.03, 29.84, 26.92, 25.94, 25.67, 25.40, 25.14, 24.87, 22.90, 22.73, 12.45. MALDI-TOF MS: calcd for ($C_{249}H_{242}N_{60}O_{45}$): m/z [M + Na]$^+$: 4815.7; found: m/z 4813.0. (EA) (%, found/calcd): C, 61.58/62.37; H, 5.29/5.09; N, 17.19/17.53.

Acknowledgements

We are grateful to the National Science Foundation of China (no. 21034006 and 21325416), and the National Fundamental Key Research Program (2011CB932702) for financial support.

Notes and references

1 (*a*) D. M. Burland, R. D. Miller and C. A. Walsh, *Chem. Rev.*, 1994, **94**, 31; (*b*) Y. Bai, N. Song, J. P. Gao, X. Sun, X. Wang, G. Yu and Z. Y. Wang, *J. Am. Chem. Soc.*, 2005, **127**, 2060; (*c*) T. J. Marks and M. A. Ratner, *Angew. Chem., Int. Ed. Engl.*, 1995, **34**, 155; (*d*) D. Yu, A. Gharavi and L. P. Yu, *J. Am. Chem. Soc.*, 1995, **117**, 11680; (*e*) S. R. Marder, B. Kippelen, A. K. Y. Jen and N. Peyghambarian, *Nature*, 1997, **388**, 845; (*f*) M. Lee, H. E. Katz, C. Erben, D. M. Gill, P. Gopalan, J. D. Heber and D. J. McGee, *Science*, 2002, **298**, 1401; (*g*) Y. Shi, C. Zhang, H. Zhang, J. H. Bechtel, L. R. Dalton, B. H. Robinson, W. H. Steier and L. R. Dalton, *Science*, 2000, **288**, 119; (*h*) C. V. M claughlin, M. Hayden, B. Polishak, S. Huang, J. D. Luo, T. D. Kim and A. K. Y. Jen, *Appl. Phys. Lett.*, 2008, **92**, 151107; (*i*) L. R. Dalton, P. A. Sullivan and D. H. Bale, *Chem. Rev.*, 2010, **110**, 25; (*j*) J. D. Luo, S. Huang, Z. W. Shi, B. M. Polishak, X. H. Zhou and A. K. Y. Jen, *Chem. Mater.*, 2011, **23**, 544; (*k*) C. Chen, X. Niu, C. Han, Z. Shi, X. Wang, X. Sun, F. Wang, Z. Cui and D. Zhang, *Opt. Express*, 2014, **22**, 19895.

2 (*a*) C. Ye and S. Fang, *Polym. Bull.*, 1990, **3**, 95; (*b*) Z. Li, Q. Li and J. Qin, *Polym. Chem.*, 2011, **2**, 2723; (*c*) W. Wu, R. Tang, Q. Li and Z. Li, *Chem. Soc. Rev.*, 2014, DOI: 10.1039/c4cs00224e.

3 (*a*) B. H. Robinson and L. R. Dalton, *J. Phys. Chem. A*, 2000, **104**, 4785; (*b*) D. Yu, A. Gharavi and L. Yu, *J. Am. Chem. Soc.*, 1995, **117**, 11680; (*c*) B. H. Robinson, L. R. Dalton, H. W. Harper, A. Ren, F. Wang, C. Zhang, G. Todorova, M. Lee, R. Aniszfeld and S. Garner, *Chem. Phys.*, 1999, **245**, 35; (*d*) K. Y. Andhya, C. K. S. Pillai and N. Tsutsumi, *Prog. Polym. Sci.*, 2004, **29**, 45; (*e*) F. Wang, A. W. Harper, M. S. Lee and L. R. Dalton, *Chem. Mater.*, 1999, **11**, 2285.

4 (*a*) L. R. Dalton, A. W. Harper and B. H. Robinson, *Proc. Natl. Acad. Sci. U. S. A.*, 1997, **94**, 4842; (*b*) M. J. Cho, D. H. Choia, P. A. Sullivan, A. J. P. Akelaitis and L. R. Dalton, *Prog. Polym. Sci.*, 2008, **33**, 1013; (*c*) S. R. Hammond, O. Clot, K. A. Firestone, D. H. Bale, D. Lao, M. Haller, G. D. Phelan, B. Carlson, A. K. Y. Jen and P. J. Reid, *Chem. Mater.*, 2008, **20**, 3425; (*d*) H. Ma and A. K. Y. Jen, *Adv. Mater.*, 2001, **13**, 1201; (*e*) J. D. Luo, S. Liu, M. Haller, L. Liu, H. Ma and A. K. Y. Jen, *Adv. Mater.*, 2002, **14**, 1763; (*f*) T. D. Kim, J. W. Kang, J. D. Luo, S. H. Jang, J. W. Ka, N. Tucker, J. B. Benedict, L. R. Dalton, T. Gray and R. M. Overney, *J. Am. Chem. Soc.*, 2007, **129**, 488; (*g*) Z. Shi, J. D. Luo, S. Huang, X. H. Zhou, T. D. Kim, Y. J. Cheng, B. M. Polishak, T. R. Younkin, B. A. Block and A. K. Y. Jen, *Chem. Mater.*, 2008, **20**, 6372.

5 (*a*) Z. Li, Z. Li, C. Di, Z. Zhu, Q. Li and Q. Zeng, *Macromolecules*, 2006, **39**, 6951; (*b*) Z. Li, Q. Zeng, Z. Li, S. Dong, Z. Zhu and Q. Li, *Macromolecules*, 2006, **39**, 8544; (*c*) Q. Li, Z. Li, Z. F. Gong, W. Z. Li and Z. Zhu, *J. Phys. Chem. B*, 2007, **111**, 508; (*d*) Q. Li, Z. Li, C. Ye and J. Qin, *J. Phys. Chem. B*, 2007, **112**, 4928; (*e*) Z. Li, S. Dong, G. Yu, Z. Li, Y. Liu and C. Ye, *Polymer*, 2007, **48**, 5520; (*f*) Z. Li, P. Li, S. Dong, Z. Zhu, Q. Li, Q. Zeng and Z. Li, *Polymer*, 2007, **48**, 3650; (*g*) Z. Zhu, Q. Li, Q. Zeng, Z. Li, Z. Li and J. Qin, *Dyes Pigm.*, 2008, **78**, 199; (*h*) Z. Li, G. Yu, S. Dong, W. Wu, Y. Liu and

C. Ye, *Polymer*, 2009, **50**, 2806; (*i*) Z. Li, W. Wu, P. Hu, X. Wu, G. Yu, Y. Liu and Z. Li, *Dyes Pigm.*, 2009, **81**, 264; (*j*) Z. Li, W. Wu, C. Ye, J. Qin and Z. Li, *J. Phys. Chem. B*, 2009, **113**, 14943; (*k*) Z. Li, Q. Zeng, G. Yu, Z. Li, C. Ye, Y. Liu and Z. Li, *Macromol. Rapid Commun.*, 2008, **29**, 136; (*l*) Q. Zeng, Z. Li, Z. Li, C. Ye, J. Qin and B. Z. Tang, *Macromolecules*, 2007, **40**, 5634; (*m*) W. Wu, Y. Fu, C. Wang, C. Ye, J. Qin and Z. Li, *Chin. J. Polym. Sci.*, 2013, **31**, 1415.

6 (*a*) H. C. Kolb, M. G. Finn and K. B. Sharpless, *Angew. Chem., Int. Ed.*, 2001, **113**, 2056; (*b*) A. Qin, J. W. Y. Lam and B. Z. Tang, *Chem. Soc. Rev.*, 2010, **39**, 2522.

7 (*a*) Z. Li, W. Wu, Q. Li, G. Yu, L. Xiao, Y. Liu, C. Ye, J. Qin and Z. Li, *Angew. Chem., Int. Ed.*, 2010, **49**, 2763; (*b*) P. A. Sullivan, H. Rommel, Y. Liao, B. C. Olbricht, A. J. P. Akelaitis, K. A. Firestone, J. W. Kang, J. Luo, J. A. Davies, D. H. Choi, B. E. Eichinger, P. J. Reid, A. Chen, A. K. Y. Jen, B. H. Robinson and L. R. Dalton, *J. Am. Chem. Soc.*, 2007, **129**, 7523.

8 (*a*) B. H. Robinson and L. R. Dalton, *J. Phys. Chem. A*, 2000, **104**, 4785; (*b*) L. R. Dalton, W. H. Steier, B. H. Robinson, C. Zhang, A. Ren, S. Garner, A. Chen, T. Londergan, L. Irwin, B. Carlson, L. Fifield, G. Phelan, C. Kincaid, J. Amend and A. K. Y. Jen, *J. Mater. Chem.*, 1999, **9**, 1905.

9 W. Wu, L. Huang, C. Song, G. Yu, C. Ye, Y. Liu, J. Qin, Q. Li and Z. Li, *Chem. Sci.*, 2012, **3**, 1256.

10 (*a*) R. Huisgen, *Angew. Chem.*, 1963, **75**, 604; (*b*) H. C. Kolb, M. G. Finn and K. B. Sharpless, *Angew. Chem., Int. Ed.*, 2001, **40**, 2004.

11 (*a*) S. Muhammad, H. L. Xu, Y. Liao, Y. H. Kan and Z. M. Su, *J. Am. Chem. Soc.*, 2009, **131**, 11833; (*b*) Y. Si and G. Yang, *J. Phys. Chem. A*, 2014, **118**, 1094; (*c*) M. R. S. A. Janjua, W. Guan, L. Yan, Z. M. Su, A. Karim and J. Akbar, *Eur. J. Inorg. Chem.*, 2010, 3466; (*d*) J. Hung, W. Liang, J. D. Luo, Z. Shi, A. K. Y. Jen and X. Li, *J. Phys. Chem. C*, 2010, **114**, 22284; (*e*) D. Sajan, I. H. Joe, J. Zaleski and V. S. Jayakumar, *Laser Phys. Lett.*, 2005, **2**, 343; (*f*) X. Li, J. Li, W. Li, X. Zhou, Q. Li, Z. Li, J. Qin and J. Hu, *Spectrochim. Acta, Part A*, 2013, **105**, 593.

12 P. Bour and T. A. Keiderling, *J. Phys. Chem. B*, 2005, **109**, 23687.

13 K. D. Singer, M. G. Kuzyk and J. E. Sohn, *J. Opt. Soc. Am. B*, 1987, **4**, 968.

